Aerodynamic Properties Identification for Small-Size Wind Turbine Blade Airfoil Sections Using the CFD Method

Saeid Fadaei[1], Robert G. Langlois, Fred F. Afagh,
[1]Carleton University
1125 Colonel By Drive, Ottawa, Canada
SaeidFadaeiNaeini@cmail.carleton.ca
RobertLanglois@cunet.carleton.ca
FredAfagh@cunet.carleton.ca

Abstract - In this paper, three airfoil sections at the root, middle, and tip of the blade of the Sunforce 400 W conventional wind turbine were investigated at different angles of attack using Computational Fluid Dynamics (CFD) to identify the stall occurrence correlated with the maximum of the lift coefficient. To verify the CFD models, firstly, simulation results of the NACA 4412 airfoil were calculated using the XFOIL code and the CFD method, and compared against available experimental data when using a k-ω SST turbulence model. Then, lift coefficients for the three airfoil sections of the small-size wind turbine blade obtained from the CFD simulations and k-ω SST turbulence model, were calculated and compared with each other. The simulations were performed at three flow speeds, V = 3, 5 and 7m/s, while the angle of attack was varied between -2 and 15 degrees until stall occurred. Flow separation occurred close to the leading edge of the airfoil at the middle and tip of the blade at lower angles of attack, while the airfoil section at the root of the blade was more successful in keeping the flow attached to the surface.

Keywords: Sunforce 400 W Conventional Wind Turbine, XFOIL, CFD, Stall Angle

1. Introduction

An airfoil is the cross-sectional form of a blade or wing utilised in a variety of applications. To generate lift, airfoils are typically constructed to provide less pressure above the wing than blow the wing. Airfoils are utilised in a broad range of applications, including wind turbine blades, axial compressor and fan blades, propellers, and wings. Airfoils play a vital part in aerodynamic applications since the aerodynamic shapes of their bodies influence their performances [1, 2]. Before any design, it is essential to select or develop the appropriate airfoil based on the application area. As a result, research has been conducted to increase the efficiencies of dynamic bodies by utilising airfoils, and numerous airfoil forms have been explored in terms of their performance [3, 4].

Cakmakcioglu et al. [5] used CFD to analyse flow over the NREL S826 airfoil at low Reynolds numbers, and the authors discovered that the results are in good agreement with existing experimental data. Likewise, Patel et al. [6] used Computational Fluid Dynamics (CFD) to study the flow around the NACA 0012 airfoil and reported that numerical simulation findings match well with experimental data. Li et al. [7] conducted a study on designing wind turbine airfoils that are used in low rated wind speed locations and found that the framework given in the study enables the design of various airfoils to meet site-specific blade requirements. Younsi et al. [8] investigated the aerodynamics of an elliptic airfoil exposed to translational and rotational motion while accounting for ground effects. They found that the majority of lift generation is due to delayed stall coupled with leading-edge vortex processes and rapid pitching. Bhat et al. [9] studied oscillating NACA 0012 airfoils at low Reynolds numbers around the stall angle and determined that leading edge vortex formation is caused by shear layer separation from the leading edge. Rostami et al. [10] studied the NACA 0012 airfoil in the presence of unstable and incompressible turbulent flows around a stationary and flapping airfoil. According to the results obtained by studying several turbulence models, nonlinear models predict a lesser stall angle than linear models. Morgado et al. [11] examined CFD and XFOIL performance predictions for high lift, low Reynolds number airfoils and discovered that XFOIL findings are comparable to CFD results. Eggert and Rumsey [12] conducted a CFD investigation on the NACA 0018 airfoil utilizing two different Reynolds-Averaged Navier-Stokes codes as well as various different turbulence models, concluding that the Shear Stress Transport (SST) and Spalart-Allmaras (SA) turbulence models generated satisfactory findings.

The performance of an airfoil at low Reynolds numbers is greatly influenced by the onset point of the boundary layer transition [13]. As a result, precisely predicting the transition zone on the surface of the airfoil is critical for understanding its performance. In this study, the flow around three airfoils, at the root, middle, and tip of a small-size conventional wind turbine blade, were investigated using the CFD method and the k-ω SST turbulence model to determine the main aerodynamic properties, particularly the stall occurrence corresponding to the maximum lift coefficient. In this respect, the NACA 4412 airfoil profile was initially taken into account, and the lift and pressure coefficients related to the stall zone were found using XFoil and CFD methods, and compared to existing experimental results.

2. XFOIL Code

The XFoil programme [14] analyses the flow around airfoils by combining a potential flow panel approach and an integrated boundary layer formulation. The algorithm was created to estimate the performance of an airfoil at low Reynolds numbers, and it achieves convergence by iterating between the outer and inner flow solutions on the boundary layer displacement thickness. For calculating the airfoil performance, the following steps are applied in XFOIL:
1. Load the coordinate data of the airfoil to XFOIL.
2. Choose the number of points used to define the airfoil.
3. Input the Reynolds number and change the fluid model inviscid to viscous.
4. Calculate the lift coefficient for a range of angles of attack between -5° and 15°.
5. Graph the lift coefficient versus angle of attack.
6. Also, graph the pressure coefficient around the airfoil and the stall angle (maximum lift coefficient).

4. CFD Method

CFD is commonly employed in a variety of applications where fluid flow is the primary consideration. The CFD approach is utilized in this work using ANSYS/Fluent to model the flow around the airfoils. The governing equations in CFD include mass, momentum, and energy conservation. The Navier-Stokes equation, commonly known as the momentum equations, is a vector equation produced by applying Newton's Law of Motion to a fluid element. It is augmented by the mass conservation equation, sometimes known as the continuity equation (mass and momentum conservation equations).

The Shear Stress Turbulence (SST) k-ω model was used to estimate the airfoil aerodynamic performance at low Reynolds numbers. Menter et al. devised the SST k-ω model, which is a two-equation eddy-viscosity model which includes turbulent kinetic energy (k) and the length scale (ω), for solving numerical problems [15, 16]. This SST formulation was created to efficiently merge the accurate k-ε model formulation in the near wall area with the free-stream correct behaviour of the k-ω turbulence closure [17].

4.1. Flow domain and grid generation

The flow domain is made up of a semicircle with a radius of 5 times and a rectangular domain with a length 10 times larger than the chord length. The airfoil is positioned in the middle of the semicircle. The boundary conditions were specified as velocity inflow and pressure at the outlet, as illustrated in Fig. 1, and the airfoil is characterized as a no slip wall. The inlet velocities were determined using the Reynolds number. The pressure and the temperature were assumed to be 1 atm and 15 °C, respectively. The atmospheric pressure is 101325 Pa, the density of the air is 1.225 kg/m^3, and the dynamic viscosity is 1.789410-5 kg/ms at this temperature.
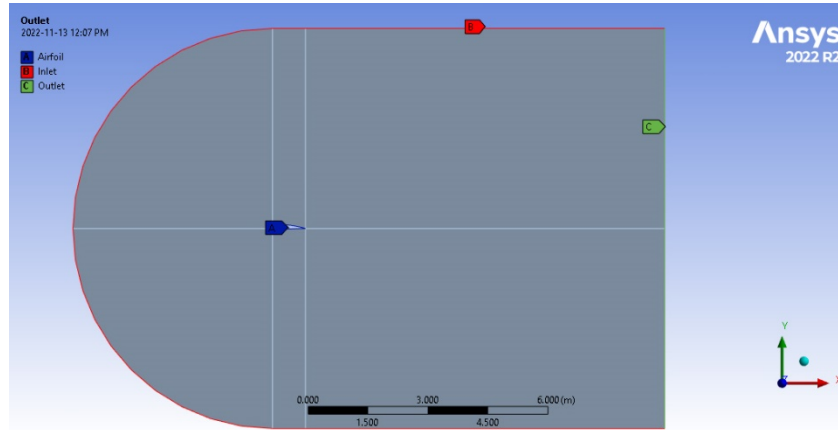
Fig. 1: Domain configuration.

To construct a structured grid, the flow domain was divided into six sections. A highly dense mesh was built around the airfoil, which is the region of interest, by determining edge sizes. All airfoils are meshed using the same size procedures and methodologies for better comparison. To appropriately calculate the flow around the airfoil, the wall y+ is maintained below 1, as required by the turbulence model. Finally, a grid with around 200000 mesh components was constructed as depicted in Fig. 2.
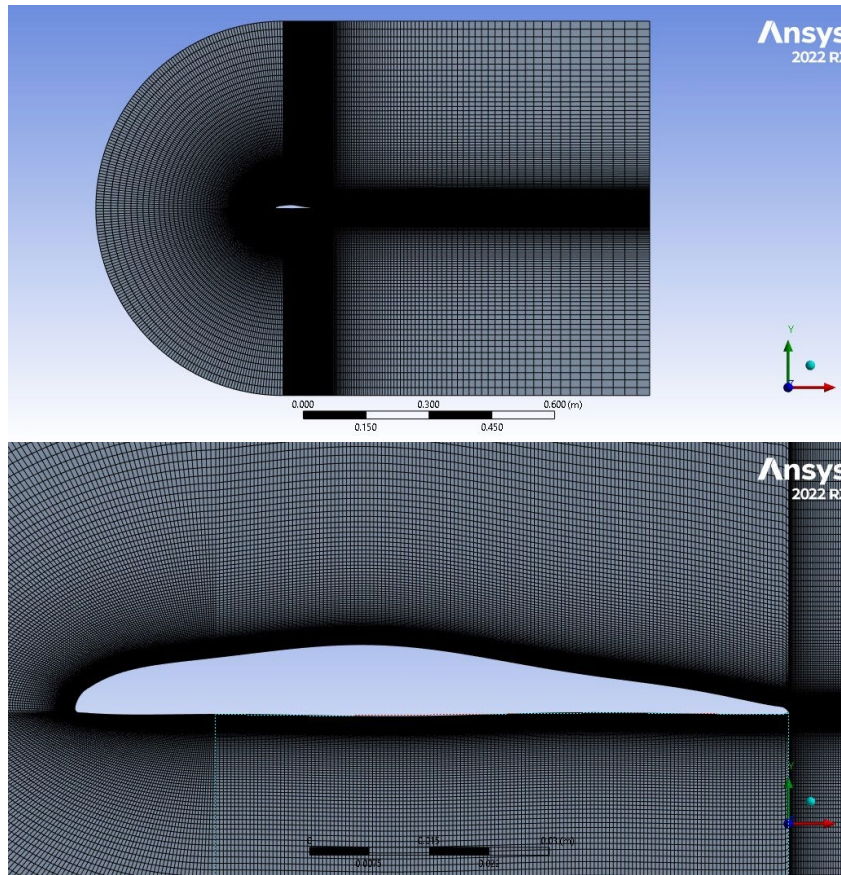

Fig. 2: Mesh model.

5. XFoil and CFD Results: NACA 4412

In order to verify the validity of the CFD technique used to calculate the aerodynamic performance of the chosen the flow performance characteristics of the NACA 4412 airfoil have been computationally evaluated at a Reynolds of 3×10^6 using ANSYS/FLUENT software with the SST k-ω turbulence model and compared to the results from the code. The comparison between the experimental studies, CFD analysis, and XFOIL code for the lift coefficient are in Fig. 3. The findings of CFD and XFOIL analyses were found to be in good agreement with the experimental results provided in the existing literature. Despite the fact that the SST k-ω turbulence model predicts slightly higher lift coefficient values, whilst XFOIL underestimates lift coefficient values, it is obvious that the XFOIL analysis tool may be utilized simply to predict aerodynamic performance of airfoils in the pre-stall and stall regions for conceptual design in engineering. The variation of pressure coefficient around the NACA4412 is provided in Fig. 4.
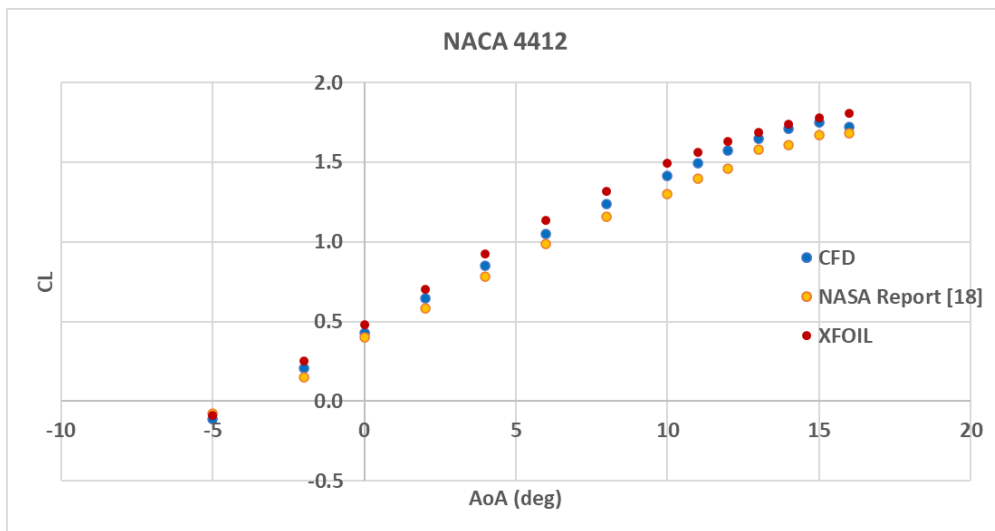

Fig. 3: Comparison of the lift coefficient of the NACA 4412 airfoil section at Re = 3×106.
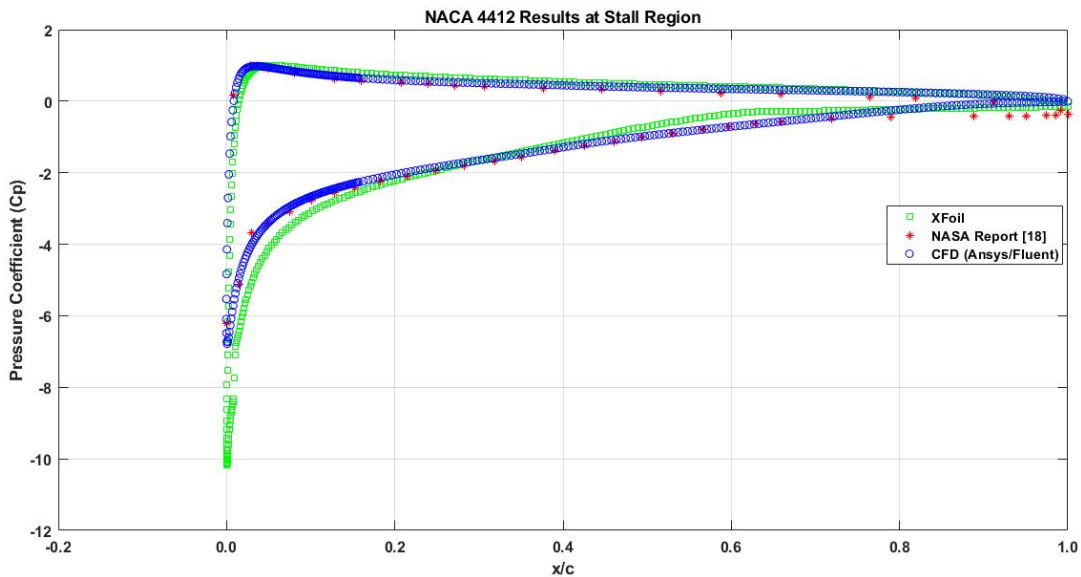

Fig. 4: Pressure coefficient around the NACA 4412 airfoil section at the stall region.

6. Airfoil Studied

As previously noted, the sections of the Sunforce 400 W conventional wind turbine that were considered were those at the tip, middle, and root of the blade. These airfoils are presented in Fig. 5.
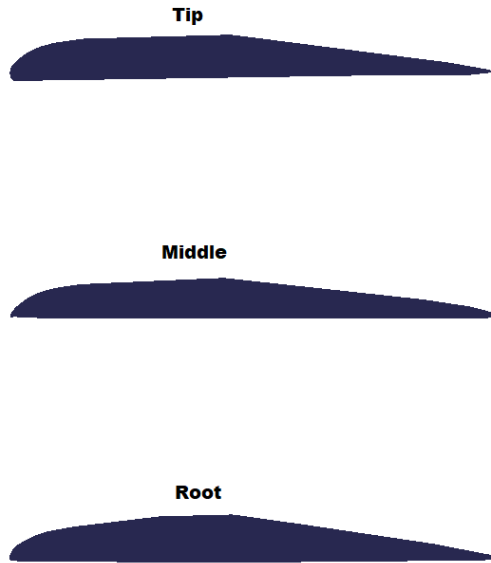
Tip

Middle

Root

Fig. 5: Airfoil sections studied.

7. Results and Discussion

Since this wind turbine was designed to operate at low wind speeds, the wind speeds corresponding to the low Reynolds number examined are V = 3 m/s and V = 5 m/s. The justification for picking these wind velocities is that this wind turbine was designed to start at an airflow speed of 3 m/s; however, it will be empirically tested at 5 m/s wind velocity in subsequent wind tunnel testing.

7.1. Airfoil Section at the Root

In Fig. 6, the results for the airfoil at the root of the aforementioned small-size wind turbine blade are presented.
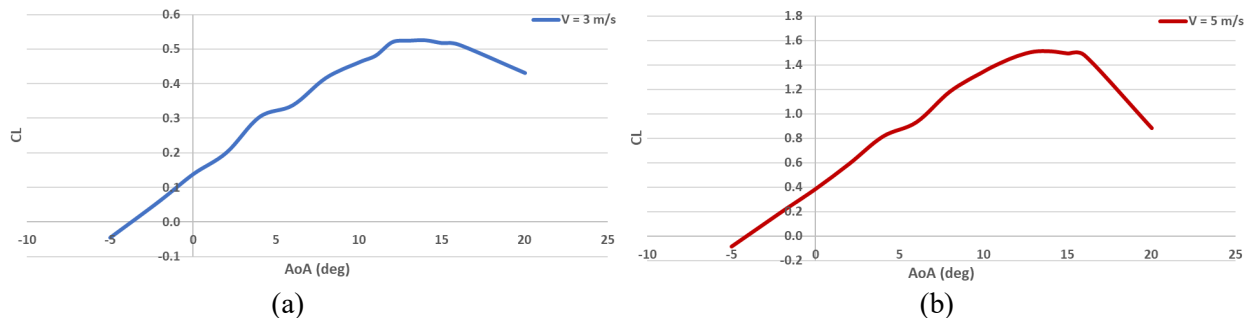
(a)

(b)

Fig. 6: Lift coefficient as a function of angle of attack at wind velocity (a) V = 3 m/s and (b) 5 m/s for the airfoil section at the root.

According to Fig. 6, stall occurs at 14 degrees of angle of attack, which corresponds to the maximum of the lift coefficient curve. The velocity contours around the airfoil at the stall are displayed in Fig. 7.
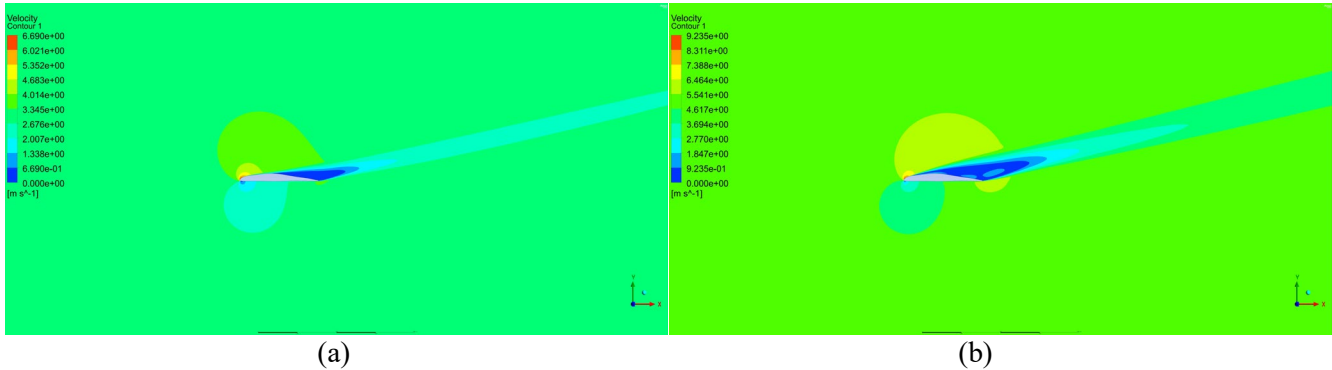
(a)　　　　　　　　　　　　　　(b)

Fig. 7: Velocity contours at an angle of attack of 14° and wind speeds of (a) V = 3 m/s and (b) V = 5 m/s.

As seen in Fig. 7, increasing the wind velocity, which is equivalent to increasing the Reynolds number, causes the stall to be more intense and the occurrence of boundary layer separation closer to the leading edge. Also, as expected, the maximum velocities at positive angles of attack were observed on the upper side of the airfoils near the leading edges and the minimum velocities at trailing edges.

7.2. Airfoil Section at the Middle and Tip

In Figs. 8 and 9, lift coefficients at different angles of attack and velocity contours corresponding to the stall region of the airfoil at the middle of the blade length are represented.
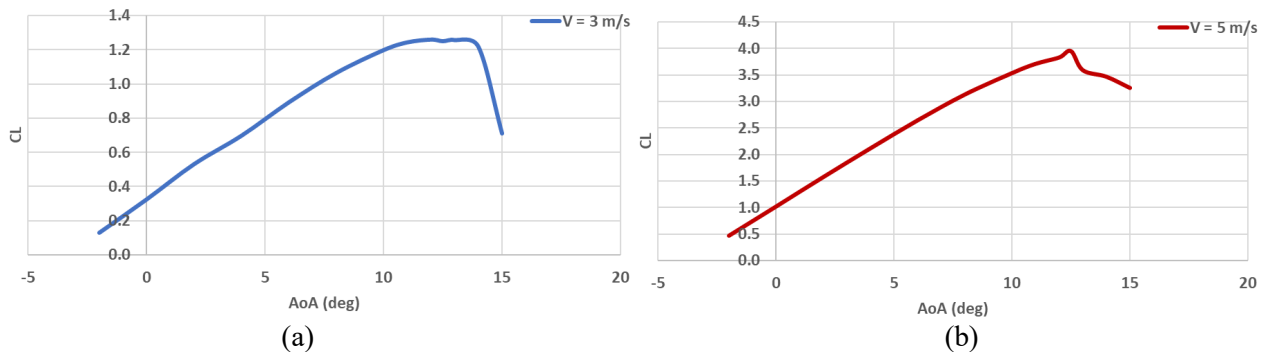

(a)　　　　　　　　　　　　　　(b)

Fig. 8: Lift coefficient of the airfoil at the mid-span of the blade at wind velocities (a) V = 3 m/s and (b) 5 m/s.
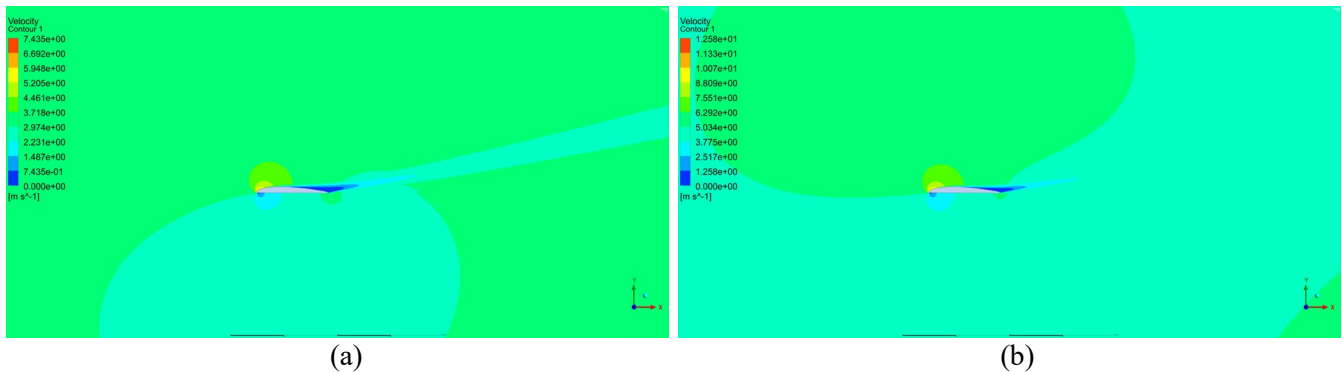

(a)　　　　　　　　　　　　　　(b)

Fig. 9: Velocity contours of the stall region for velocities (a) V = 3 m/s and (b) V = 5 m/s.

It can be seen that the airfoil at the mid-span of the blade stalls at lower angles of attack of 13.0 and 12.5 degrees compared with the airfoil section at the root of the blade at both wind speeds V = 3 m/s and 5 m/s, respectively. Similarly, the lift coefficients of the airfoil at the tip of the blade with increasing angle of attack is shown in Fig. 10.
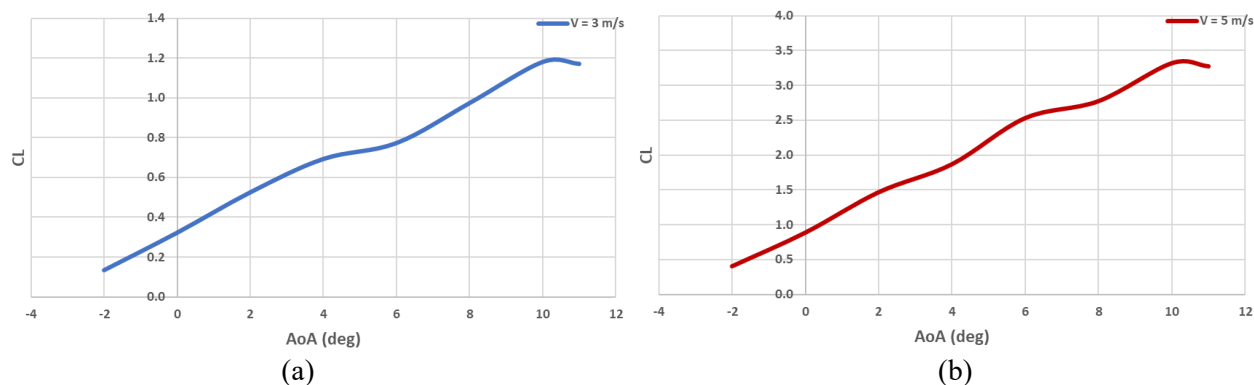

(a)   (b)

Fig. 10: Lift coefficient at the tip of the blade at wind velocities of (a) V = 3 m/s and (b) 5 m/s.

The airfoil at the tip of the blade obviously stalls at lower angles of attack, and as wind speed increases, the lift coefficient increases which leads to stall at lower angles of attack.

8. Conclusion
The aerodynamic performance of three airfoils at different radial positions along a small-size conventional wind turbine blade were examined using the CFD approach in this work. First, the NACA 4412 airfoil CFD solution and XFOIL results were compared to available experimental data, and it was discovered that numerically-simulated results are in good agreement with experimentally-obtained values. Lift coefficients generated from CFD simulations are found to be very close to experimental data, although XFOIL results are slightly lower than published data. As expected, according to the flow simulation results, lift coefficients usually increase as the angle of attack increases up to a specific point, is called stall, that corresponds to the maximum lift coefficient. Stalls, in general, reduce the aerodynamic performance of airfoils at the specified angle of attack. For wind speed V = 3 m/s, the airfoil at the root experiences stall at roughly 14° degrees angle of attack, whereas this occurs at 13° and 10° degrees for airfoils in the middle and tip of the blade, respectively. Increasing wind speed leads to stall occurrence at lower angles of attack.

References
[1]   C. Tarhan and I. Yilmaz, "Numerical and experimental investigations of 14 different small wind turbine airfoils for 3 different reynolds number conditions," *Wind Struct.*, vol. 28, no. 3, pp. 141–153, 2019, doi: https://doi.org/10.12989/was.2019.28.3.141.
[2]   A. Alonso-Estebanez, J. J. del Coz Diaz, F. P. . lvarez Rabanal, P. Pascual-Munoz, and P. J. G. Nieto, "Numerical investigation of truck aerodynamics on several classes of infrastructures," *Wind Struct.*, vol. 26, no. 1, pp. 35–43, 2018, doi: https://doi.org/10.12989/was.2018.26.1.035.
[3]   E. Basta, M. Ghommem, L. Romdhane, and A. Abdelkefi, "Modeling and experimental comparative analysis on the performance of small-scale wind turbines," *Wind Struct.*, vol. 30, no. 3, pp. 261–273, 2020, doi: https://doi.org/10.12989/was.2020.30.3.261.
[4]   M. O. Tasci, I. Karasu, and B. Sahin, "Investigation of crossflow features of a slender delta wing," *Wind Struct.*, vol. 31, no. 3, pp. 229–240, 2020.
[5]   S. C. Cakmakcioglu, I. O. Sert, O. Tugluk, and N. Sezer-Uzol, "2-D and 3-D CFD Investigation of NREL S826 Airfoil at Low Reynolds Numbers," *J. Phys. Conf. Ser.*, vol. 524, p. 012028, Jun. 2014, doi: 10.1088/1742-6596/524/1/012028.

[6]   K. S. Patel, S. B. Patel, U. B. Patel, and A. P. Ahuja, "CFD Analysis of an Aerofoil," *Int. J. Eng. Res.*, vol. 3, no. 3, pp. 154–158, 2014.

[7]   X. Li, L. Zhang, J. Song, F. Bian, and K. Yang, "Airfoil design for large horizontal axis wind turbines in low wind speed regions," *Renew. Energy*, vol. 145, pp. 2345–2357, Jan. 2020, doi: 10.1016/j.renene.2019.07.163.

[8]   A. Younsi, A. abdellah el-hadj, S. zamree bin abd Rahim, and T. Rezoug, "Aerodynamic investigation of an airfoil under two hovering modes considering ground effect," *J. Fluids Struct.*, vol. 91, p. 102759, Nov. 2019, doi: 10.1016/j.jfluidstructs.2019.102759.

[9]   S. S. Bhat and R. N. Govardhan, "Stall flutter of NACA 0012 airfoil at low Reynolds numbers," *J. Fluids Struct.*, vol. 41, pp. 166–174, Aug. 2013, doi: 10.1016/j.jfluidstructs.2013.04.001.

[10]   M. J. V. Rostami, M. Saghafian, A. Sedaghat, and M. Miansari, "Numerical investigation of turbulent flow over a stationary and oscillatory NACA0012 airfoil using overset grids method," *Int. J. Numer. Methods Fluids*, vol. 67, no. 2, pp. 135–154, Sep. 2011, doi: 10.1002/fld.2332.

[11]   J. Morgado, R. Vizinho, M. A. R. Silvestre, and J. C. Páscoa, "XFOIL vs CFD performance predictions for high lift low Reynolds number airfoils," *Aerosp. Sci. Technol.*, vol. 52, pp. 207–214, May 2016, doi: 10.1016/j.ast.2016.02.031.

[12]   C. A. Eggert and C. L. Rumsey, "CFD Study of NACA 0018 Airfoil with Flow Control," 2017. [Online]. Available: https://ntrs.nasa.gov/citations/20170004500.

[13]   P. V. Gamboa and M. A. R. Silvestre, "Airfoil optimization with transition curve as objective function," in *VI International Conference on Adaptive Modelling and Simulation ADMOS*, 2013, pp. 1–12.

[14]   M. Drela, "XFOIL: An Analysis and Design System for Low Reynolds Number Airfoils," 1989, pp. 1–12.

[15]   P. M. Gresho, "Some current CFD issues relevant to the incompressible Navier-Stokes equations," *Comput. Methods Appl. Mech. Eng.*, vol. 87, no. 2–3, pp. 201–252, Jun. 1991, doi: 10.1016/0045-7825(91)90006-R.

[16]   F. R. Menter, "Influence of freestream values on k-omega turbulence model predictions," *AIAA J.*, vol. 30, no. 6, pp. 1657–1659, Jun. 1992, doi: 10.2514/3.11115.

[17]   C. D. Argyropoulos and N. C. Markatos, "Recent advances on the numerical modelling of turbulent flows," *Appl. Math. Model.*, vol. 39, no. 2, pp. 693–732, Jan. 2015, doi: 10.1016/j.apm.2014.07.001.

[18]   I. H. Abbott, A. E. Von Doenhoff, and J. Stivers, Louis, "Summary of Airfoil Data," 1945.